

Supporting Information for:

**Fluorescent Excimers and Exciplexes of the Purine Base Derivative**

**8-Phenylethynylguanine in DNA Hairpins**

Kristen E. Brown, Arunoday P. N. Singh, Yi-Lin Wu, Lin Ma, Ashutosh K. Mishra, Brian T. Phelan,  
Ryan M. Young\*, Frederick D. Lewis\*, Michael R. Wasielewski\*

*Department of Chemistry, Argonne-Northwestern Solar Energy Research (ANSER) Center, and Institute  
for Sustainability and Energy at Northwestern, Northwestern University, Evanston, Illinois 60208-31131*

\*Corresponding author: [ryan.young@northwestern.edu](mailto:ryan.young@northwestern.edu), [fdl@northwestern.edu](mailto:fdl@northwestern.edu),  
[m-wasielewski@northwestern.edu](mailto:m-wasielewski@northwestern.edu)

## Contents

<b>Time-Resolved Spectroscopy .....</b>	S-2
<i>Experimental Details .....</i>	S-2
<i>Data Analysis .....</i>	S-3
<b>Additional Characterization and DFT Calculations .....</b>	S-4
<b>Additional Time-Resolved Spectroscopy Measurements .....</b>	S-8
<i>Fluorescence Up-Conversion Spectroscopy .....</i>	S-9
<i>Femtosecond Transient Absorption Spectroscopy .....</i>	S-10
<i>Femtosecond Stimulated Raman Spectroscopy .....</i>	S-14
<b>Raman Mode Assignments .....</b>	S-17
<b>References for Supporting Information .....</b>	S-18

## Time-Resolved Spectroscopy

### Experimental Details

*Transient Absorption Spectroscopy.* The details of our femtosecond transient absorption (fsTA) apparatus are detailed elsewhere.<sup>1</sup> Briefly, the ~100 fs output of regeneratively amplified Ti:sapphire laser (Spectra-Physics Tsunami/Spitfire) is split into two fractions to form the pump and probe beams. Specifically, a portion of the 827 nm fundamental (~50 µJ/pulse) was directed onto an 8 ns delay stage before being tightly focused into a 3 mm sapphire crystal to generate probe continuum ranging from 420 nm to 850 nm. NIR (800-1600 nm) continuum generation was accomplished by softly focusing the fundamental into a proprietary crystal (Ultrafast Systems, LLC). The probe is split using a neutral density filter so that one portion interacts with the sample and one portion provides a reference spectrum. ~400 µJ/pulse of the fundamental was directed into a non-collinear optical parametric amplifier (TOPAS-White, Light-Conversion, LLC.) which was used to generated the 350 nm pump (second harmonic signal). The pump was attenuated and sent through a commercial depolarizer (DPU-25-A, Thorlabs, Inc.) to suppress the effects of rotational dynamics and chopped at 500 Hz. The reference and the transmitted probe beams were coupled into optical fibers and detected using a customized Helios spectrometer (Ultrafast Systems, LLC). Nanosecond transient absorption (nsTA) experiments were conducted using the same femtosecond laser to generate the 350 nm excitation pulses at 1 kHz and using the ultrabroadband (360-1600+ nm) output of a photonic crystal fiber pumped by a Nd:YAG laser operating at 2 kHz was used as the probe (Eos, Ultrafast Systems, LLC).

*Femtosecond Stimulated Raman Spectroscopy (FSRS).* The details of our femtosecond stimulated Raman spectroscopy apparatus are also given elsewhere.<sup>2</sup> The actinic pump (350 nm, 35 fs) and narrowband (480 nm, ~2 ps) beams are overlapped with a ~100 fs broadband continuum probe. Interaction of the Raman pump and probe with the sample initiate the vibrational coherence with high temporal specificity relative to the actinic pump delay, resulting in high temporal (~150 fs) and frequency (~15 cm<sup>-1</sup>) resolution. The Raman pump energy was maintained at 500 nJ/pulse.

## Data Analysis

*Data Treatment.* Prior to kinetic analysis, the fsTA and FSRS data are background/scatter-subtracted and chirp-corrected, and the visible and NIR data sets are spectrally merged (Surface Xplorer 4, Ultrafast Systems, LLC). Kinetic data from the fluorescence up-conversion experiment are temporally smoothed with 5-point adjacent averaging prior to fitting. For FSRS data, the electronic background signals are removed by subtracting a spline-fit baseline anchored on either side of each Raman feature, after subtraction of the ground state/solvent peaks,<sup>2</sup> or by fitting a low order polynomial to  $\sim 500 \text{ cm}^{-1}$  regions of the data individually and then merged. Because the background is species-dependent and follows the kinetic evolution of the transient states, the spline subtraction is done at each time delay using the same frequencies, but with the y-axis (gain) values allowed to vary. Typically greater than 40 points were used in the spline-fit. The resulting background-subtracted FSRS spectra are spectrally smoothed with 5-point adjacent averaging prior to presentation.

*Single-Wavelength Analysis.* Single-wavelength fluorescence up-conversion kinetic analysis is performed in Origin 2015 by fitting the time-dependent signals  $S(t)$  to the convolution of Gaussian instrument response with temporal width  $w$  and (i) a multi-exponential decay with amplitudes  $a_i$  and time constants  $\tau_i$ , (ii) a delta function with amplitude  $a_0$ , centered at the zero of pump-probe delay ( $t_0$ ) to account for instrument-limited coherence artifacts, and (iii) offsets for before ( $S_0$ ) and after ( $S'_0$ )  $t_0$  to account for any signals present beyond the experimental window:

$$S(t) = e^{-t^2/w^2} * \begin{cases} S_0 & t < t_0 \\ S'_0 + a_0\delta(t - t_0) + \sum_{i=1}^N a_i \exp[-(t - t_0)/\tau_i] & t \geq t_0 \end{cases} \quad (\text{Eqn. S1})$$

The time-resolution is given as  $2w\sqrt{\ln 2} = 300 \text{ fs}$  (full width at half maximum, FWHM).

*Global Analysis.* The global kinetic analysis was performed using home written programs in MATLAB and was based on a global fit to selected wavelengths/frequencies. Each wavelength/frequency is given an initial amplitude that is representative of the spectral intensity at time  $t_0$ , and varied independently to fit the data. The time/rate constants and  $t_0$  are shared between the various kinetic traces and are varied globally across the kinetic data in order to fit the model(s) described in the text. We globally fit the dataset to a set of pre-specified

mathematical functions convoluted with the instrument response and use the resultant populations to deconvolute the dataset and reconstruct decay-associated spectra:

$$S(\lambda, t) = \sum_n A_n(\lambda, 0) \exp[-t / \tau_n], \quad (\text{Eqn. S2})$$

where  $n$  can vary between 1 and 5. The MATLAB program convolutes the equations with a Gaussian instrument response function with FWHM = 300 fs before employing a least-squares fitting using a Levenberg-Marquardt or Simplex method to find the parameters which result in matches to the kinetic data. Each function corresponds to a given population with a well-defined temporal evolution. The raw data matrix is then deconvoluted with the fitted populations as functions of time to produce the spectra associated with each mathematical component,  $A_n(\lambda, 0)$ .

### **Additional Characterization and DFT Calculations**

**Table S1.**  $m/z$  values for oligomer sequences determined by MALDI-TOF mass spectrometry. Melting temperature of hairpins and capped hairpins were measured in 10 mM phosphate buffer + 100 mM NaCl at pH 7.2.

<b>Sample</b>	<b><math>m/z</math></b>		<b><math>T_m</math></b> (°C)
	<b>calculated</b>	<b>found</b>	
<b>EG-T</b>	4656.24	4658	40
<b>EG-C</b>	4661.14	4663	>80
<b>EG-A</b>	4656.24	4658	39
<b>EG-G</b>	4661.14	4664	>80
<b>EG-Z</b>	4660.16	4663	>80
<b>EG<sub>2</sub></b>	4761.28	4763	>80
<b>EG<sub>3</sub></b>	5479.72	5483	>80

**Figure S1.** HPLC chromatogram of purified samples, RP C18 column, and gradient of 8-28% CH<sub>3</sub>CN in 30 mM TEAA buffer.

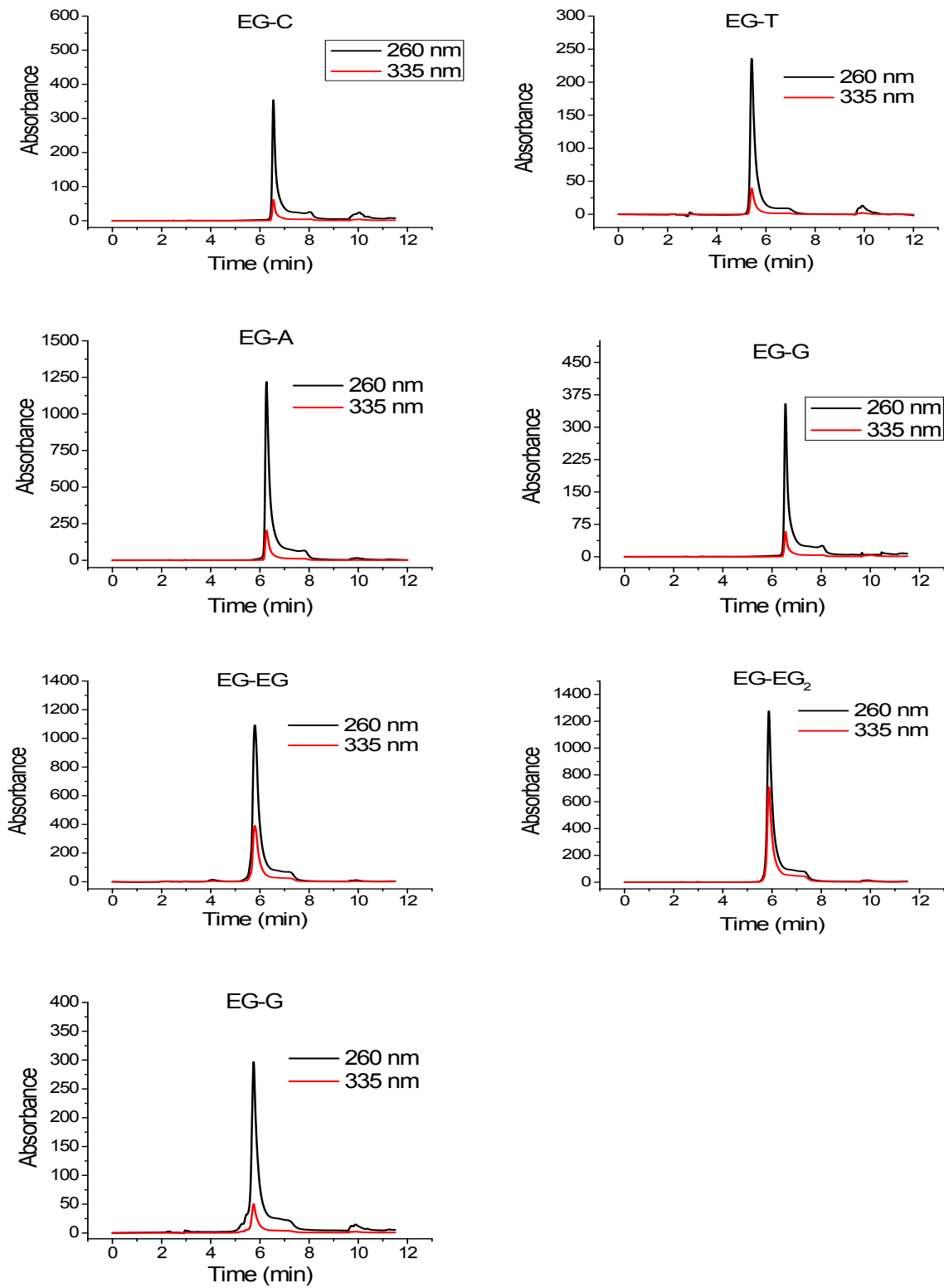


**Figure S2.** (a) Normalized absorption and (b) fluorescence spectra of nucleotide **EG-H<sub>2</sub>** in several solvents and (c) unnormalized fluorescence spectra with fluorescence quantum yields.

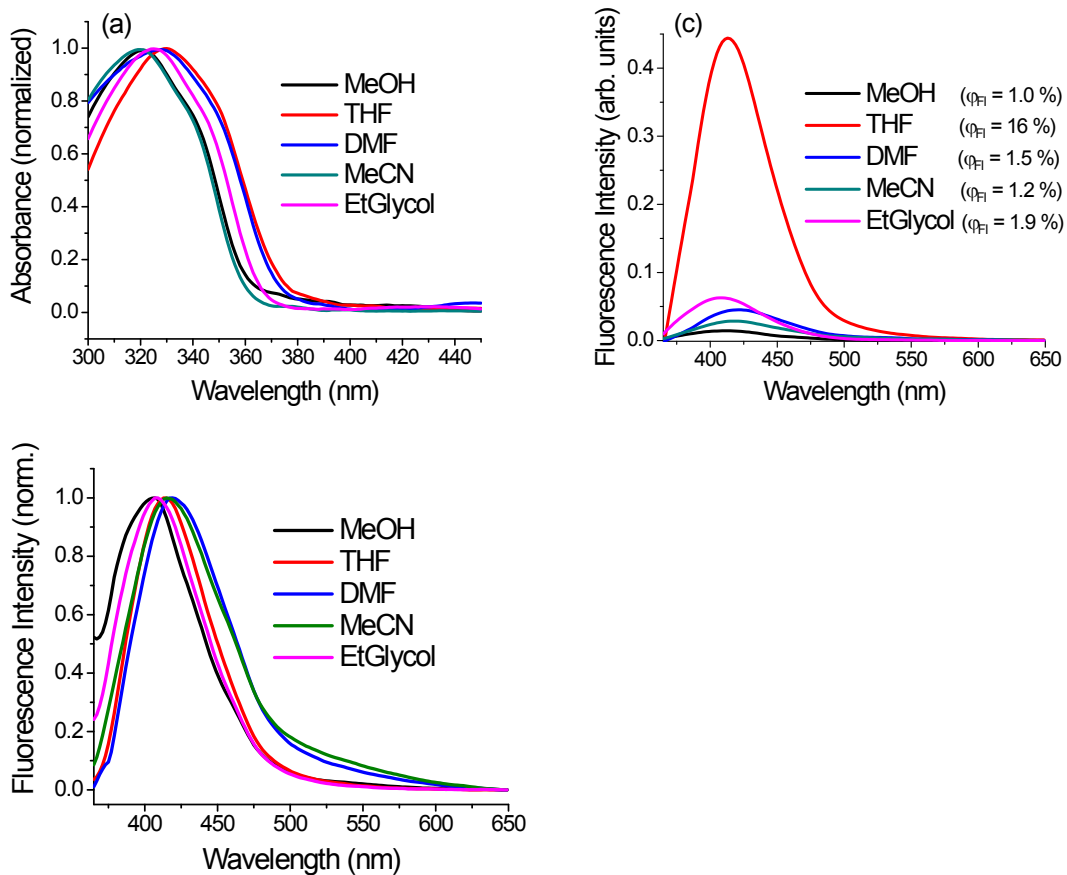


**Figure S3.** (a) Highest occupied and (b) lowest unoccupied molecular orbitals and (c) calculated absorption spectra with a bandwidth of 0.33 eV showing lowest energy transitions of 8-(4'-phenylethynyl)guanine obtained using TD-DFT calculations at the B3LYP/6-31G(d) level.<sup>3</sup>

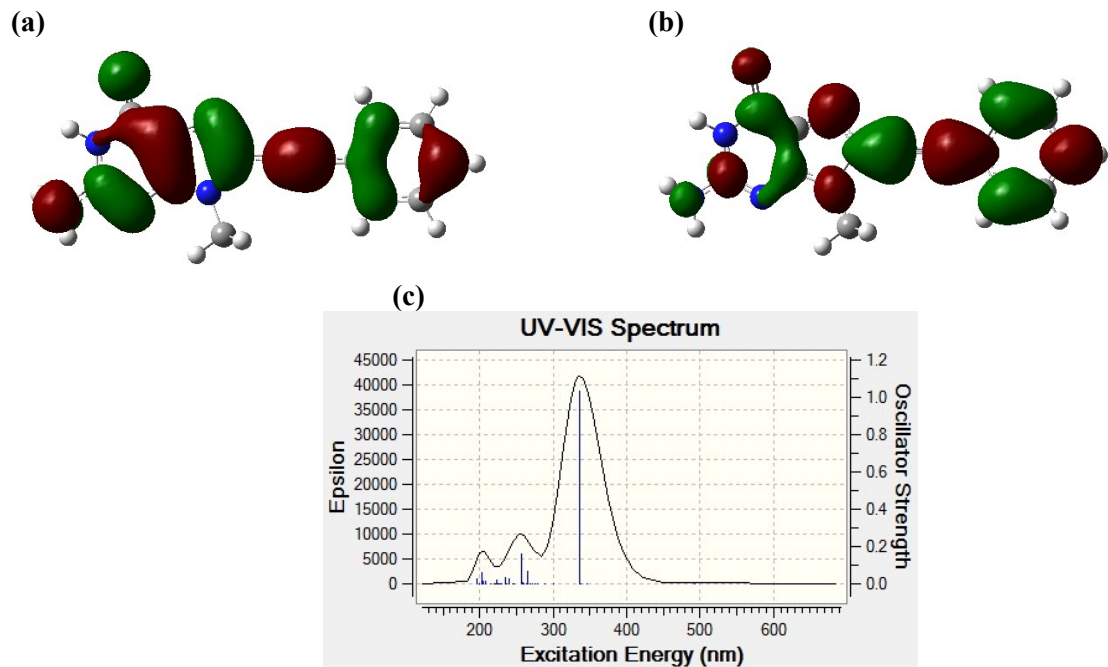


**Table S2.** Summary of the first twenty singlet transitions.

Excited State	Energy (eV)	Wavelength (nm)	Oscillator Strength $f$
1	3.6826	336.68	1.0331
2	4.5523	272.35	0.0012
3	4.665	265.78	0.0678
4	4.782	259.27	0.0029
5	4.8399	256.17	0.1605
6	5.0174	247.11	0.0003
7	5.0716	244.47	0.0005
8	5.1556	240.49	0.0015
9	5.1561	240.46	0.0267
10	5.2891	234.41	0.0314
11	5.5566	223.13	0.016
12	5.575	222.39	0.0008
13	5.7511	215.58	0.0001
14	5.9472	208.48	0.0074
15	5.9649	207.86	0.0133
16	6.068	204.32	0.0138
17	6.0876	203.67	0.0583
18	6.1076	203	0.0487
19	6.2173	199.42	0.0002
20	6.3050	196.64	0.0252

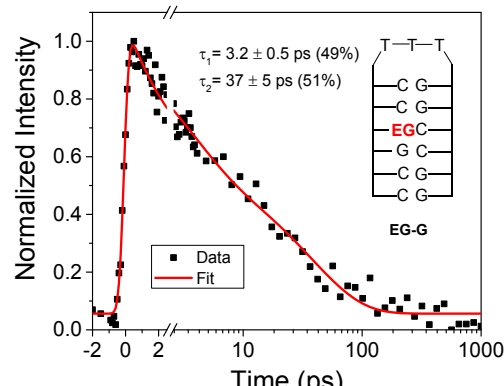
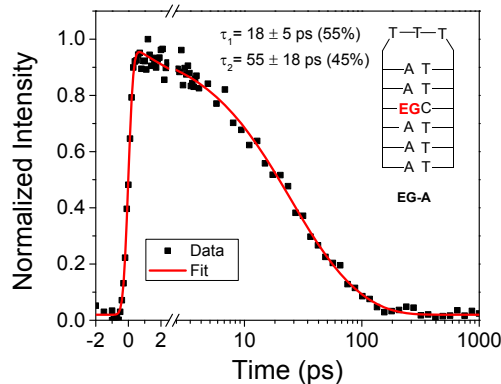
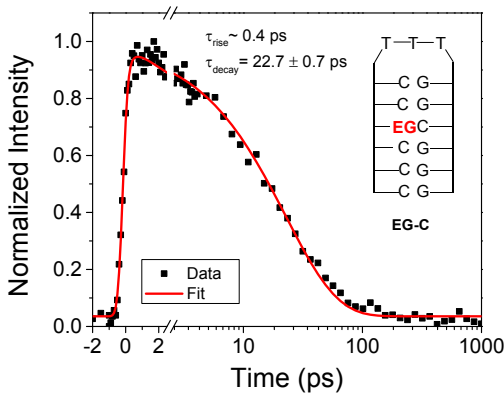
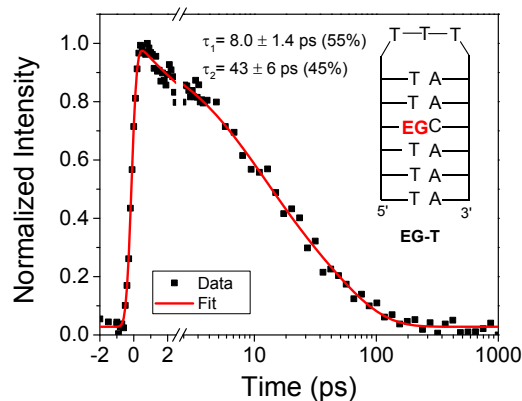
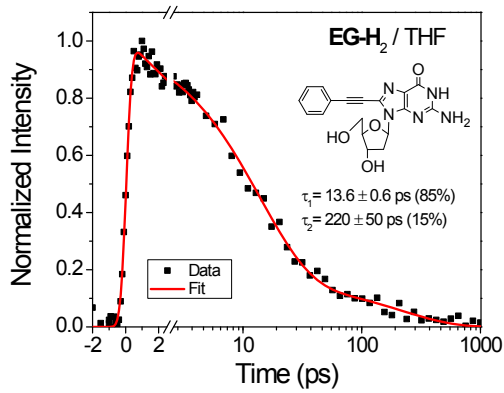
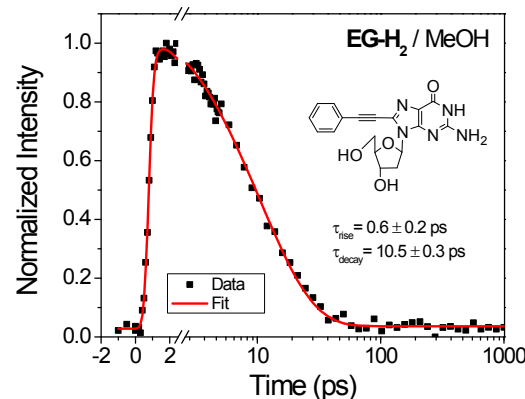
**Table S3.** Geometry for TD-DFT calculation.

Atom	X	Y	Z
N	-4.60652	0.676644	0.004272
C	-4.51987	-0.69177	0.001461
N	-3.38321	-1.34739	-0.01108
C	-2.30192	-0.526	-0.00179
C	-2.26213	0.873632	-0.00858
C	-3.50544	1.604468	-2.6E-05
N	-0.97243	1.33164	-0.00947
C	-0.22728	0.236472	-0.00456
N	-0.99737	-0.93209	-0.00013
C	1.183079	0.185398	-0.004
C	2.398082	0.121906	-0.00288
H	-5.51108	1.127462	0.085365
O	-3.73477	2.800232	0.011548
N	-5.70593	-1.39085	0.067684
H	-5.58482	-2.38104	-0.10464
H	-6.50566	-0.99163	-0.40743
C	3.820905	0.087522	-0.00143
C	4.559428	1.288635	-0.00335
C	5.950736	1.255666	-0.00176
C	6.628454	0.033614	0.001712
C	5.904844	-1.16159	0.003633
C	4.513136	-1.1402	0.002089
H	4.028478	2.235328	-0.00595
H	6.509015	2.187839	-0.00319
H	3.948615	-2.0677	0.003697
H	6.42725	-2.11442	0.00643
C	-0.52008	-2.30436	0.009055
H	0.097571	-2.49953	-0.87255
H	0.072564	-2.49732	0.90825
H	-1.39214	-2.95966	-0.00177
H	7.714728	0.012783	0.002987

## Additional Time-Resolved Spectroscopy Measurements

### Fluorescence Up-Conversion Spectroscopy

**Figure S4.** Fluorescence decays for **EG-H<sub>2</sub>** in MeOH and THF, and **EG-T**, **-C**, **-A** and **-G** in aqueous buffer. Samples were excited at  $\lambda_{\text{ex}} = 320 \text{ nm}$  (10 nJ/pulse) and emission was detected at  $\lambda_{\text{em}} = 430 \text{ nm}$ . All time constants refer to decays unless explicitly noted.



## Femtosecond Transient Absorption Spectroscopy

**Figure S5.** Transient absorption, decay-associated spectra, and single-wavelength decays of EG-H<sub>2</sub> in aqueous buffer solution (10 mM phosphate buffer + 100 mM NaCl at pH 7.2), THF, and MeCN following 350 nm (1  $\mu$ J/pulse) excitation.

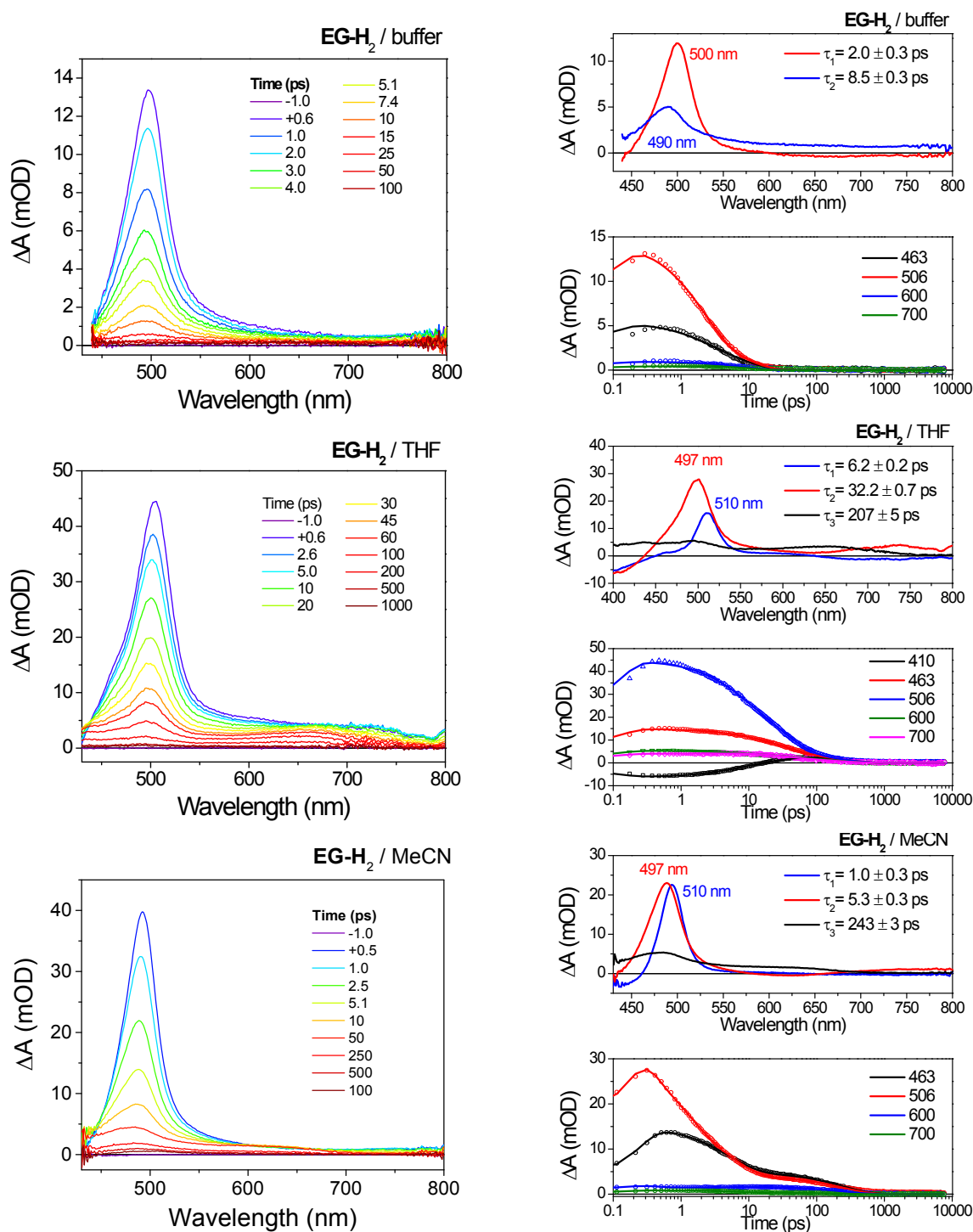


**Figure S6.** Transient absorption, decay-associated spectra, and single-wavelength decays of **EG-T**, **EG-C**, and **EG-A** in aqueous buffer solution (10 mM phosphate, 0.1 M NaCl, pH 7.2) following 350 nm (1  $\mu$ J/pulse) excitation.

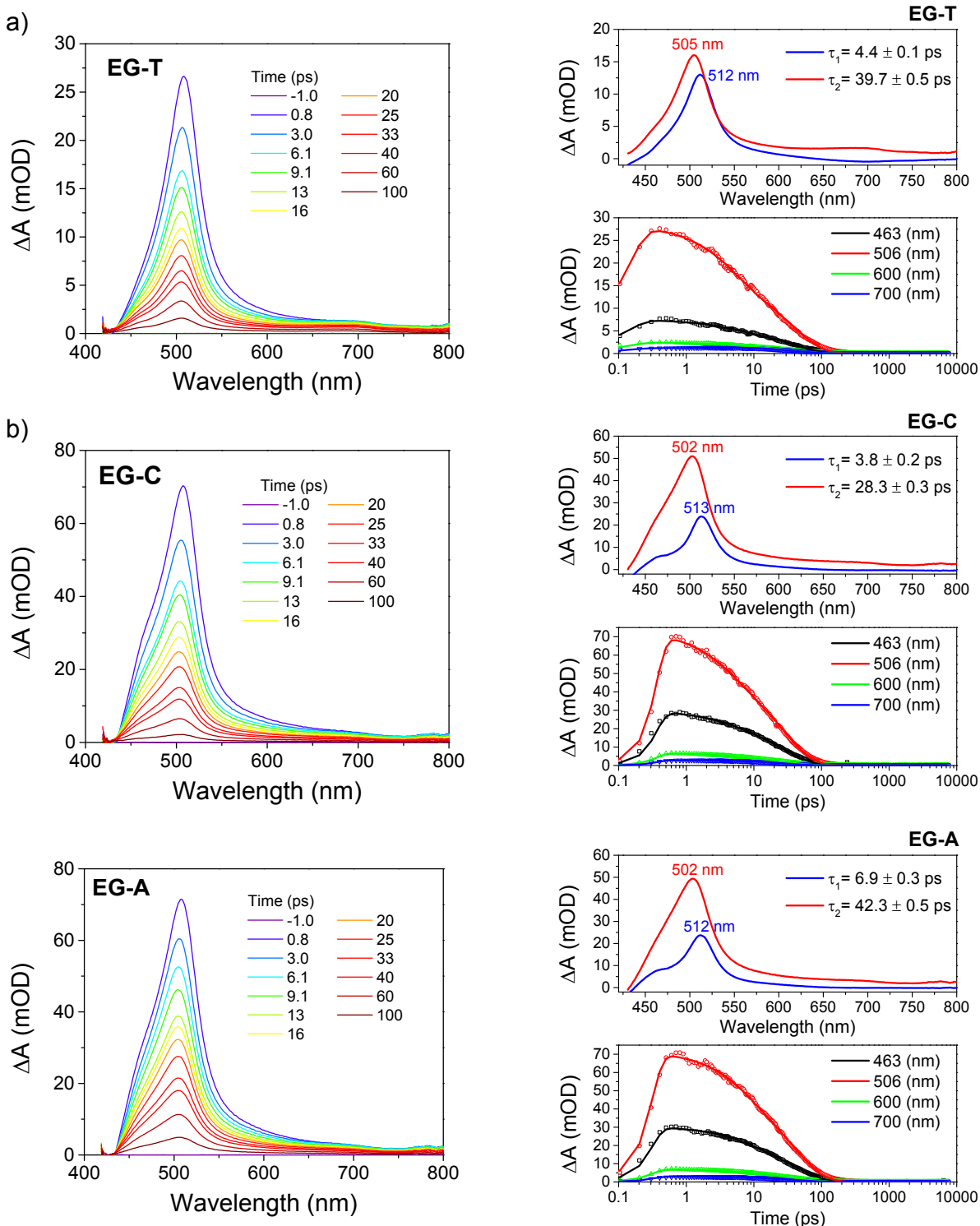


**Figure S7.** Transient absorption, decay-associated spectra, and single-wavelength decays of **EG-G** and **EG-Z** in aqueous buffer solution (10 mM phosphate, 0.1 M NaCl, pH 7.2) following 350 nm (1  $\mu$ J/pulse) excitation.

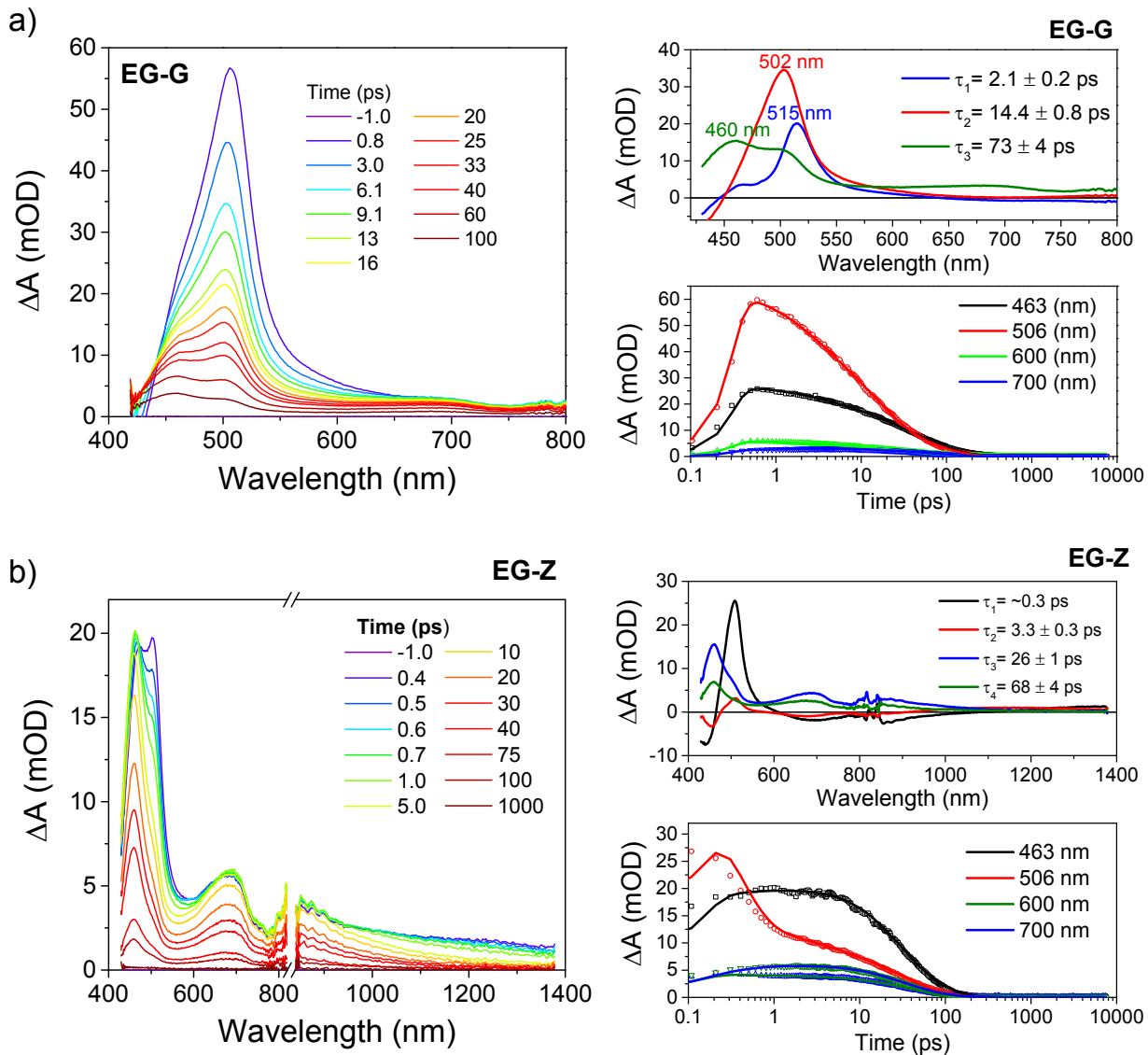
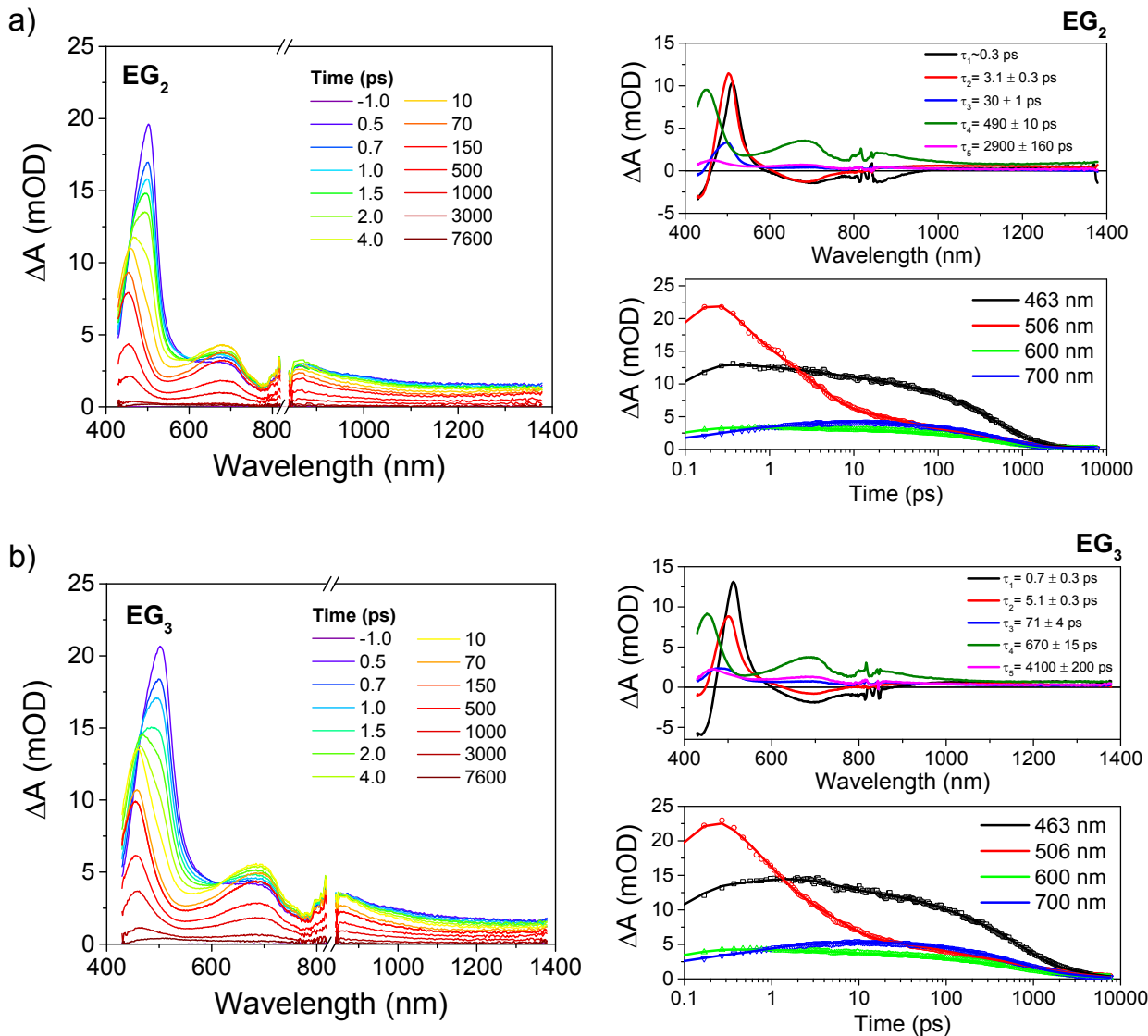


**Figure S8.** Transient absorption, decay-associated spectra, and single-wavelength decays of **EG<sub>2</sub>** and **EG<sub>3</sub>** in aqueous buffer (10 mM phosphate, 0.1 M NaCl, pH 7.2) following 350 nm (1  $\mu$ J/pulse) excitation.



## Femtosecond Stimulated Raman Spectroscopy

**Figure S9.** Femtosecond stimulated Raman spectra of (a) **EG-H<sub>2</sub>** in MeOH and (b) **EG-G** in aqueous buffer following 350 nm actinic excitation and collected using a 480 nm Raman pump. Also shown are decay-associated spectra following multi-frequency global fitting and single-frequency decay kinetics. Other hairpins were not sufficiently stable under Raman conditions to obtain full time-resolved data sets.

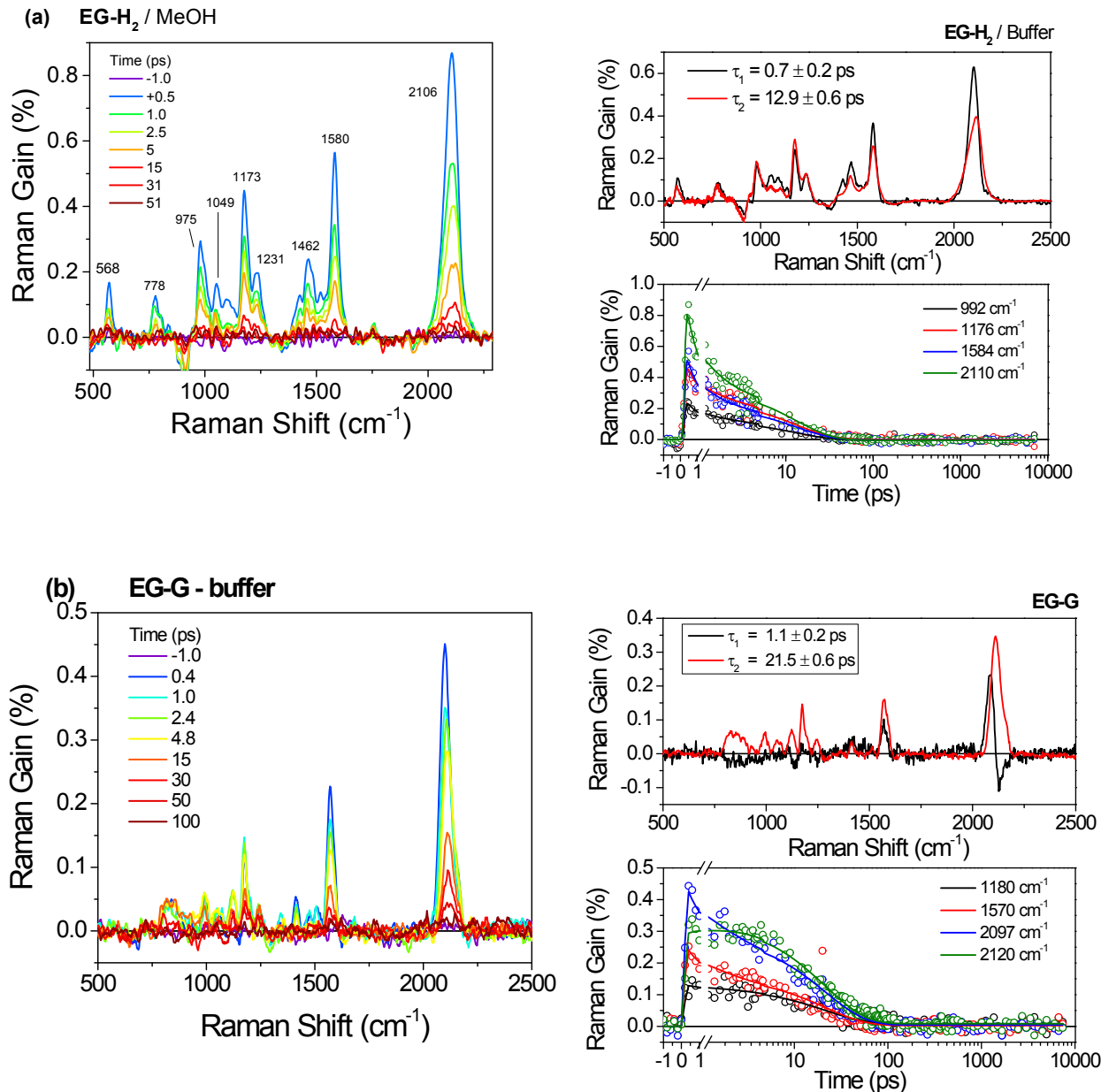


**Figure S10.** Comparison of the normalized FSRS spectra of **EG-C**, **-G**, **-Z**, and **EG<sub>2</sub>** at 25 ps.

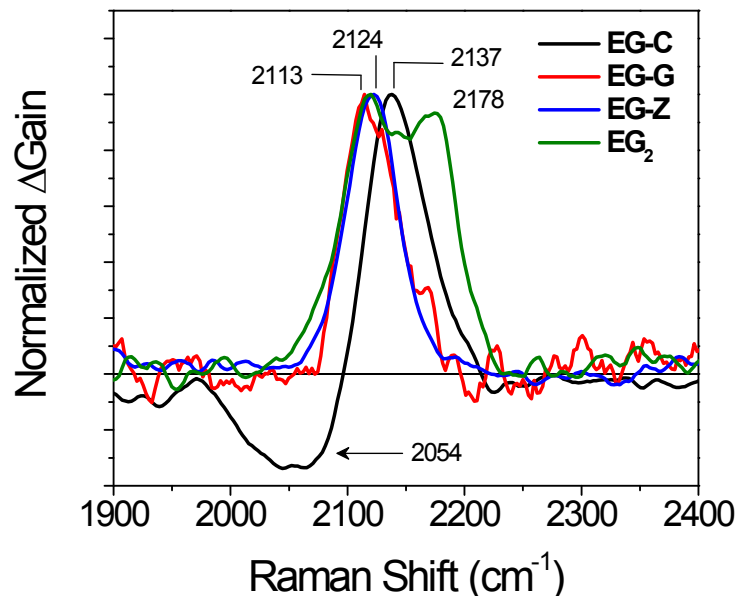


**Figure S11.** Comparison of the FSRS spectrum for **EG-H<sub>2</sub>** ( $\lambda_{AP} = 350$  nm,  $\lambda_{RP} = 480$  nm) at  $\Delta t = 1.0$  ps (blue) to DFT-calculated Raman spectrum of <sup>1\*</sup>EG with 15 cm<sup>-1</sup> Lorentzian broadening (black). For clarity, the calculated Raman spectrum is normalized to the 1580 cm<sup>-1</sup> mode for shifts < 1800 cm<sup>-1</sup>, and to the 2100 cm<sup>-1</sup> mode for shifts > 1800 cm<sup>-1</sup>.

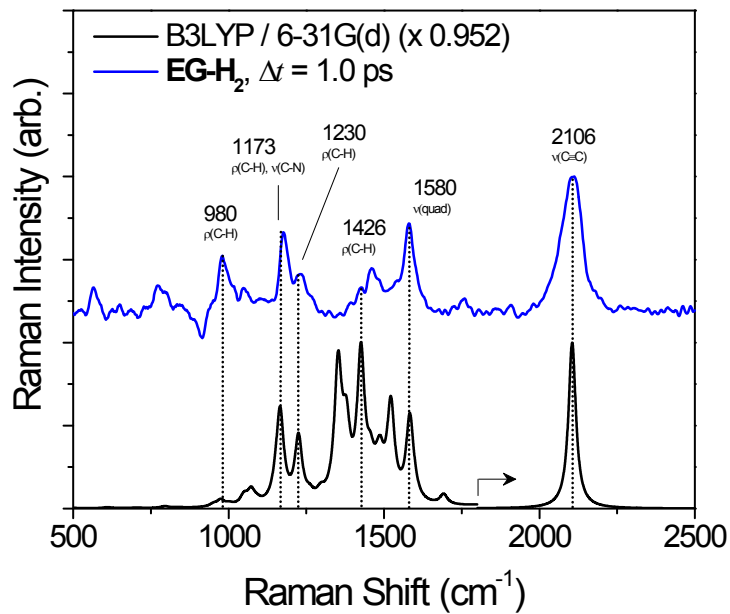


**Figure S12.** Comparison of the ethynyl stretching region of the FSRS spectra for **EG**<sub>2</sub> ( $\lambda_{AP} = 350$  nm,  $\lambda_{RP} = 480$  nm) in the excimer state at  $\Delta t = 56$  ps with **EG**<sub>2</sub> in the local-excited (LE) state at  $\Delta t = 1$  ps (red curve), and the spectrum of the phenylethylnylguanine cation **EG**<sup>+</sup> adapted from reference S4 (blue curve).<sup>4</sup>

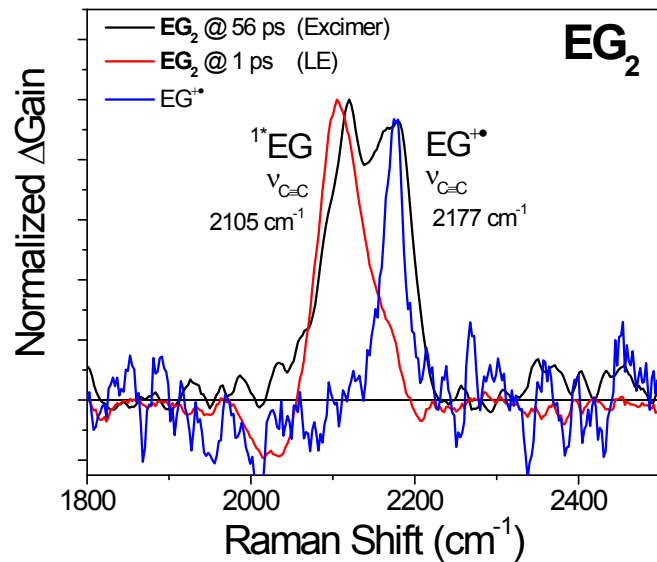
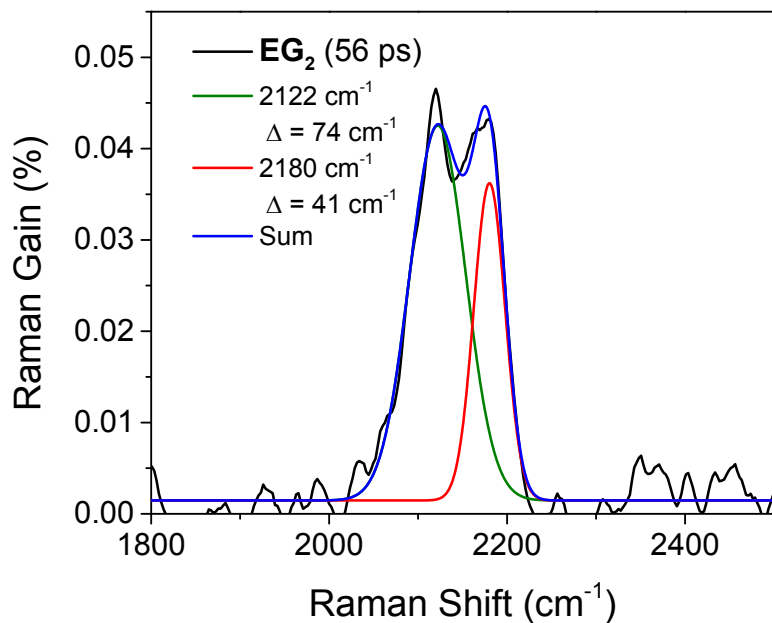


**Figure S13.** Gaussian decomposition of the Raman spectrum for **EG**<sub>2</sub> ( $\lambda_{AP} = 350$  nm,  $\lambda_{RP} = 480$  nm) at  $\Delta t = 56$  ps (black) supporting the band assignments discussed in caption for Figure S11.



## Raman Mode Assignments

**Table S4.** Selected Raman Peak Assignment for  ${}^1\text{E}\text{G}$  adapted from Reference S4.

Exp. ( $\text{cm}^{-1}$ )	Strength	Calc ( $\text{cm}^{-1}$ )	Intensity ( $\text{\AA}^4/\text{amu}$ )	Assignment	Mode
980	M	1023.2	$8.46 \times 10^4$	$\rho(\text{C-H})$ (phenyl)	
1173	S	1224.6	$1.30 \times 10^6$	$\rho(\text{C-H})$ (phenyl) $\nu(\text{C-N})$ (guanine)	
1230	S	1286.6	$9.37 \times 10^5$	$\rho(\text{C-H})$ (phenyl) $\nu(\text{N-H})$ (guanine)	
1426	M	1497.9	$2.04 \times 10^6$	$\rho(\text{C-H})$ (phenyl)	
1580	W	1662.8	$1.20 \times 10^6$	$\nu_{\text{quad}}$ , (phenyl)	
2104	S	2211.5	$1.79 \times 10^7$	$\nu_{\text{C}\equiv\text{C}}$	

TD-DFT / B3LYP; 6-31G(d), scaling factor: 0.952. W = weak; M = medium; S = strong.

## **References for Supporting Information**

1. R. M. Young, S. M. Dyar, J. C. Barnes, M. Juríček, J. F. Stoddart, D. T. Co and M. R. Wasielewski, *J. Phys. Chem. A*, 2013, **117**, 12438-12448.
2. K. E. Brown, B. S. Veldkamp, D. T. Co and M. R. Wasielewski, *J. Phys. Chem. Lett.*, 2012, **3**, 2362-2366.
3. M. J. Frisch, G. W. Trucks, H. B. Schlegel, G. E. S. M. A. Robb, J. R. Cheeseman, G. Scalmani, V. Barone and G. A. Petersson, *Gaussian 09*, (2009) Gaussian, INC, Wallingford CT.
4. K. E. Brown, A. P. N. Singh, Y.-L. Wu, A. K. Mishra, J. Zhou, F. D. Lewis, R. M. Young and M. R. Wasielewski, *J. Am. Chem. Soc.*, 2017, <http://pubs.acs.org/doi/10.1021/jacs.1027b06998>.